

Cite this: *Org. Biomol. Chem.*, 2014, **12**, 589

Azacalix[2]arene[2]triazine-based receptors bearing carboxymethyl pendant arms on nitrogen bridges: synthesis and evaluation of their coordination ability towards copper(II)[†]

João M. Caio,^{a,b} Teresa Esteves,^b Sílvia Carvalho,^a Cristina Moiteiro*^b and Vítor Félix*^a

For functional nitrogen-bridged calix(hetero)aromatic platforms to be further used in the design of more sophisticated receptors, the azacalix[2]arene[2]triazine nitrogen bridges were functionalised with methyl bromoacetate. Three new macrocycles with four *N*-methyl ester pendant arms were straightforwardly prepared in good yields from the undecorated azacalix[2]arene[2]triazine precursors with chlorine, dimethylamine or dihexylamine substituted triazines. These intermediate macrocycles exhibited different reactivity towards the nucleophilic replacement, which was rationalized from the computed electrostatic potential for these molecules. Subsequently, the *N*-methyl ester appendages were hydrolyzed with each dialkylamine derivative providing a single macrocycle with four carboxylic groups. In contrast, the hydrolysis of the dichlorinated azacalix[2]arene[2]triazine analogue yielded a mixture of three isomeric macrocycles having two *N*-methyl esters and two carboxymethyl pendant arms and the triazine chlorine atoms replaced by hydroxyl groups. The coordination ability of two macrocycles with four carboxylic groups for transition metals was evaluated with copper(II) by UV-vis titrations.

Received 13th October 2013,
Accepted 11th November 2013

DOI: 10.1039/c3ob42047g

www.rsc.org/obc

Introduction

1,3,5-Triazine derivatives have found widespread application in medicinal chemistry, herbicides, catalysis, textiles, dyestuffs and optical bleaches, among others.¹ In the area of supramolecular chemistry, the 1,3,5-triazine derivatives have been extensively used as a central building unit of sophisticated architectures including organic and inorganic–organic hybrid frameworks.^{1a,2} Moreover, the 1,3,5-triazine-based compounds containing both donor and acceptor hydrogen binding sites are able to form self-assemblies by a network of complementary intermolecular hydrogen bonds eventually assisted by π -interactions.³ It is also noteworthy that 1,3,5-triazine is a

versatile building block straightforwardly obtained from the highly reactive cyanuric chloride, which is commercially available as a low-cost material.^{1a}

The intermolecular interactions mentioned above have also inspired the supramolecular chemistry community for the design of macrocyclic receptors containing a 1,3,5-triazine ring^{4,5} as the recognition entity of charged^{3,6} or neutral substrates^{7–9} with biological relevance. These receptors include several macrocyclic platforms decorated with 1,3,5-triazine units such as classical calixarenes^{10–12} or common cyclam derivatives.¹³ Alternatively, the triazine units are incorporated into the macrocyclic framework as illustrated by azacalix[2]arene[2]triazine derivatives where four aromatic units composed of two phenyl and two triazine rings are commonly arranged in a 1,3-alternate fashion. These azacalix[*n*]-heteroarenes were originally reported by Wang *et al.*¹⁴ and are promptly obtained by two successive S_NAr coupling reactions between electrophilic-activated cyanuric chloride units and nucleophilic 1,3-phenyldiamine derivatives. The same group also showed that the replacement of the *N*-bridged hydrogen atoms by bulky groups such as alkyl, methyl, benzyl or *p*-methoxyphenyl substituents leads to the fine tuning of azacalix[2]arene[2]triazine cavity size and shape due to the perturbation caused by these substituents on the conjugation state of the nitrogen bridging atoms.¹⁵ Besides the appendage of substituents at the

^aDepartamento de Química, CICECO and Secção Autónoma de Ciências da Saúde, Universidade de Aveiro, 3810-193 Aveiro, Portugal. E-mail: vitor.felix@ua.pt;

Fax: +351 234 370 084

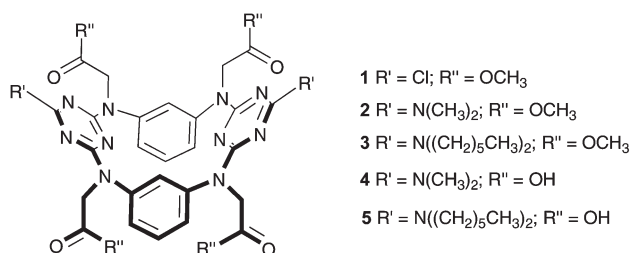
^bDepartamento de Química e Bioquímica and Centro de Química e Bioquímica, Faculdade de Ciências, Universidade de Lisboa, Campo Grande, 1749-016 Lisboa, Portugal. E-mail: cmmoiteiro@fc.ul.pt; Fax: +351 217 500 088

[†]Electronic supplementary information (ESI) available: ¹H and ¹³C NMR spectra, IR data, MS (ESI) spectra, HRMS (ESI) data of all compounds, UV-vis titration data for 4 and 5 and crystallographic data of 1, 2 and 12 including the corresponding ORTEP diagrams and CIF files. CCDC 957200, 957201 and 957202. For ESI and crystallographic data in CIF or other electronic format see DOI: 10.1039/c3ob42047g

nitrogen bridges, the azacalix[2]arene[2]triazine platform can be easily functionalized through the replacement of the two labile triazine chlorine atoms or by the introduction of the binding units at phenyl rings.^{8,15}

In spite of the chemical versatility, the inherent hydrogen bonding capacity and π acidic character of the azacalix[2]arene[2]triazine scaffold, as aforementioned, the use of this entity remains almost unexplored concerning the design of functional synthetic receptors for charged or neutral guest species. In contrast, the dichlorinated tetraoxacalix[2]arene[2]triazine macrocycle is able to host inorganic polyatomic anions with different geometries through the anion- π interactions established with both electron deficient triazine rings,¹⁶ while the S_NAr replacement of both chlorine atoms by chelating pyridine amines leads to macrocycles with highly selective coordination ability for copper(II).¹⁷ On the other hand, binding studies with azacalix[2]arene[2]triazine derivatives are limited. Recently, macrocycles incorporating this platform were obtained by functionalization of the upper rim with L-alanine units, and their molecular recognition ability towards aromatic carboxylate anions was evaluated by our groups.⁶ Furthermore, a HPLC stationary phase based on tetraazacalix[2]arene[2]triazine-modified silica gel was prepared and further used in the separation of various polycyclic aromatic hydrocarbons, nitrobenzene, organic bases, phenols, and inorganic anions.¹⁸ This platform anchored to a silica supporter was also applied as an SPE sorbent for the extraction of trace-level tobacco-specific N-nitrosamines in plasma matrices.¹⁹

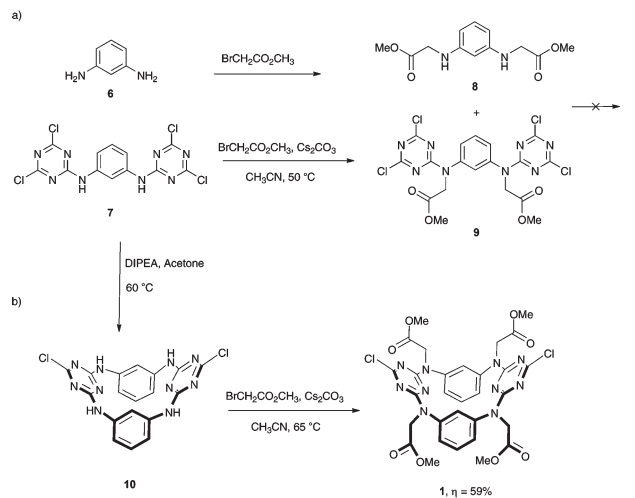
Pursuing our research line in exploring the azacalix[2]arene[2]triazine as a platform for the appendage of binding units, herein, we report the functionalization of the nitrogen bridges with ester methyl groups leading to a new series of macrocycles 1–5. The ester groups were hydrolyzed and the coordination ability of the carboxylic acid derivatives 4 and 5 was evaluated for transition metals with copper(II). The recognition capability of these receptors for neutral substrates is illustrated with the X-ray crystal structure of macrocycle 1 with the diglycolic acid.



Results and discussion

Synthesis

In order to prepare the azacalix[2]arene[2]triazine derivative 1, two synthetic strategies were initially intended as shown in Scheme 1.



Scheme 1 Two synthetic pathways (a and b) devised for the synthesis of *N,N,N,N*-tetracarboxymethylazacalix[2]arene[2]triazine 1.

The synthetic route (a), requires the functionalization of starting materials *m*-phenylenediamine 6 and the trimer 7, with methyl bromoacetate before the macrocyclization reaction. The trimer 7 was previously obtained by the reaction of 6 with two high reactive cyanuric chloride molecules, as earlier described by Wang *et al.*¹⁴ The derivatization of the starting material 6 was undertaken using different bases (Cs₂CO₃ or K₂CO₃), temperatures (room or 65 °C) and solvents (DMF, CH₃CN or THF). In these experimental conditions, the intermediates 8 and 9 were always obtained together with several secondary products, as it was impossible to separate them from the crude reaction mixture. In spite of the separation failing, and in order to obtain 1 through the synthetic pathway (a), we have decided to continue the reaction between the crude products 8 and 9. However, the formation of the macrocycle 1 was not observed, which led us to definitively leave this synthetic approach.

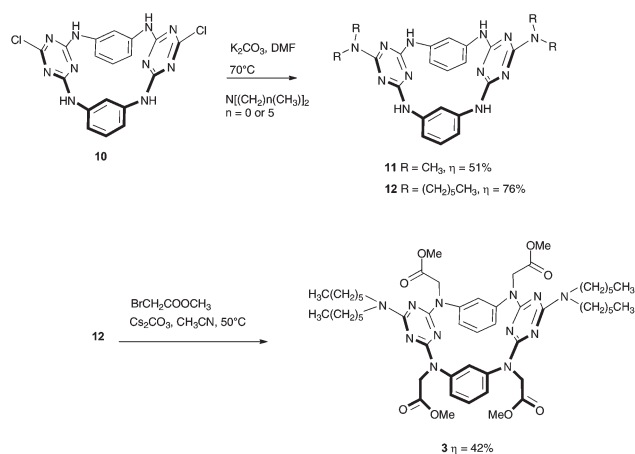
Alternatively, in the synthetic route (b), the macrocyclic platform azacalix[2]arene[2]triazine 10 was synthesized from the coupling reaction between 6 and the trimer 7 in 58% yield using experimental conditions slightly modified from those previously reported by Wang *et al.*¹⁴ Afterwards, the *N*-H bridging groups of 10 were functionalized with methyl bromoacetate (10 eq.) in CH₃CN/Cs₂CO₃, yielding the target *N*-tetramethyl ester macrocycle 1 in 59% yield. The insertion of four methyl ester appendages at the nitrogen bridges was confirmed by the ¹H NMR spectrum through the absence of a singlet corresponding to the four *N*-H bridges at δ 10.00 ppm and the occurrence of two new singlets at δ 4.47 and 3.75 ppm assigned to four methylene and methoxy groups, respectively. Furthermore, the four *N*-methyl ester-bridging groups were corroborated by the ¹³C NMR spectrum with a resonance at δ 169.7 ppm and by the IR spectroscopy through a band at 1750 cm⁻¹ assigned to carbonyl groups. The ESI-MS spectrum showed a [M + H]⁺ ion peak at *m/z* 727 and an adduct ion [M + Na]⁺ at *m/z* 749 was also consistent with the existence of 1. The subsequent MS² spectrum of the [M + H]⁺ showed the loss

of CH_3OH , one and two fragments of $\text{C}(\text{OH})^+\text{OCH}_3$ from *N*-methyl ester arms. The presence of two chlorine-substituted triazines was confirmed by $[\text{M} + 2]^+$ and $[\text{M} + 4]^+$ ion peaks with relative intensities 64/10, reflecting the natural isotope distribution pattern of chlorine $^{35}\text{Cl}/^{37}\text{Cl}$. The structure of **1** was further established by single crystal X-ray diffraction, which revealed the existence of an unexpected dimethyl diglycolate molecule associated with **1**, *vide infra*. The dimethyl diglycolate is a side reaction product eventually derived from the basic assisted self-condensation of two methyl bromoacetate molecules along the appending reaction.

Aiming at the potential use of tetra-carboxylic acid derivatives as eventual intermediates in organic synthesis, the lipophilicity of the azacalix[2]arene[2]triazine platform was changed, replacing the chlorine atoms of the triazine rings by two dialkylamines with different alkyl size chains (dimethylamine or dihexylamine). The substitution of two electron-withdrawing groups by two electron-donating groups leads necessarily to azacalix[2]arene[2]triazine derivatives with different reactivity on the nitrogen bridges.

Bearing in mind these considerations, the syntheses of the ester macrocycles **2** and **3** were undertaken following two synthetic pathways. In the first route (Scheme 2), the appending reaction of methyl ester arms was preceded by the preparation of the dialkyl amine derivatives **11** and **12** through the replacement of the triazine chlorine atoms of **10** by dimethyl- and dihexylamine, respectively. The success of these two nucleophilic reactions was corroborated by the ^1H NMR spectra of **11** and **12**, displaying chemical shifts between δ 3.63–3.10, 1.71–1.20 and 0.94–0.93 ppm assigned to NCH_2 , $-(\text{CH}_2)_4-$ alkyl **12** and CH_3 terminal chains respectively. The formation of **11** was confirmed by ESI-MS spectrum with a $[\text{M} + \text{H}]^+$ ion peak at m/z 457 while the evidence of **12** was obtained by TOF-MS exhibiting a $[\text{M}]^+$ ion peak at m/z 737. In addition, the structure of **12** was definitively established by single crystal X-ray structure determination, *vide infra*.

In order to obtain the target macrocycles **2** and **3**, the intermediates **11** and **12** were subsequently reacted in acetonitrile

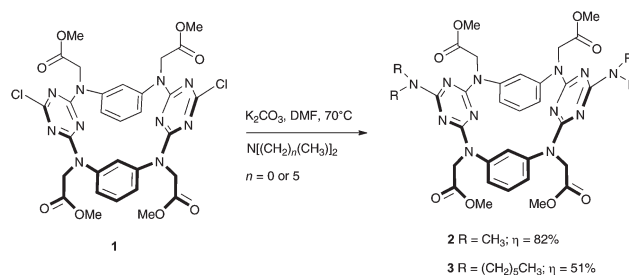


Scheme 2 Synthesis of the target macrocycle **3** preceded by the replacement of both chlorine atoms of **10** by dialkylamines.

with methyl bromoacetate in the presence of Cs_2CO_3 using different equivalents (10 to 20 eq.) of these two reagents (Scheme 2). The target **3**, with two dihexylamine chains, was successfully obtained from **12** in 42% yield when 16 equivalents of both Cs_2CO_3 and methyl bromoacetate were used. The formation of **3** was confirmed through the ^1H NMR spectrum, showing a multiplet at δ 4.35 ppm and a singlet at δ 3.69 ppm assigned to the methylene and methoxy groups respectively, both from the four *N*-methyl ester arms. In agreement, the ESI-MS spectrum performed in positive ion mode showed a $[\text{M} + \text{H}]^+$ ion peak at m/z 1026 and an adduct ion $[\text{M} + \text{Na}]^+$ at 1048. Furthermore, the macrocycle **3** exhibits a fragmentation pattern similar to **1**.

In contrast, the intermediate **11** did not afford the macrocycle **2** using equivalent reaction conditions. Thus, the reactivity of **12** seems to be related with the higher solubility of this intermediate in acetonitrile, considering that **11** and **12** have comparable reactivity towards the nucleophilic substitution reaction as later discussed. It is noteworthy that the insertion of the *N*-methyl ester appendages was successful only when acetonitrile was used as a solvent.

Alternatively, in the second synthetic route (Scheme 3), the macrocycles **2** and **3** are obtained directly from the *N*-tetramethyl ester derivative **1**. Thus, **2** was prepared by the reaction of **1** with dimethylamine in the presence of K_2CO_3 and DMF at 70°C in a yield of 82%. The ^1H NMR spectrum of **2** compared with **1** shows a new singlet at δ 3.05 ppm assigned to four NCH_3 methyl groups. The ESI-MS spectrum exhibits a $[\text{M} + \text{H}]^+$ ion peak at m/z 745 consistent with the molecular formula of **2**. The structure of **2** was further corroborated by single crystal X-ray diffraction, *vide infra*. Compound **3** was also obtained using identical experimental conditions in a yield of 51%, which represents a slight improvement relative to the synthetic approach outlined in Scheme 2. Therefore, these experimental results seem to indicate that the NH bridging units in the undecorated macrocycle **10** are more reactive towards the nucleophilic substitution than the dialkylamine substituted triazines **11** and **12**. Further insights into the reactivity of N–H bridging groups were obtained from the calculation of the electrostatic potential on the surfaces of **10–12** using the Hartree–Fock computational analysis as follows.



Scheme 3 Synthesis of **2** and **3** directly from **1** after the insertion of carboxymethyl pendant arms on nitrogen bridges of the parent macrocycle **10**.

Electronic structure calculations

The electrostatic potential computed on a molecule's electron density surface (V_s) provides an effective tool to evaluate non-covalent interactions, which are largely electrostatic in nature.²⁰ In particular, the most positive values ($V_{s,max}$) and the most negative values ($V_{s,min}$) of V_s have been shown to correlate well with hydrogen-bond acidity and basicity respectively.^{21,22} Therefore, we decided to assess the $V_{s,max}$ and $V_{s,min}$ for macrocycles **10–12** in order to rationalize their reactivity in

Table 1 $V_{s,max}$ (left) and $V_{s,min}$ (right) values (kcal mol⁻¹). On the 0.001 electron per bohr³ density surfaces of **10–12**

10	11	12
44.6, -35.5	35.5, -49.9	35.8, -50.7
44.2, -35.4	35.3, -49.7	35.4, -50.4
43.8	34.5	34.1
43.8	34.4	33.9

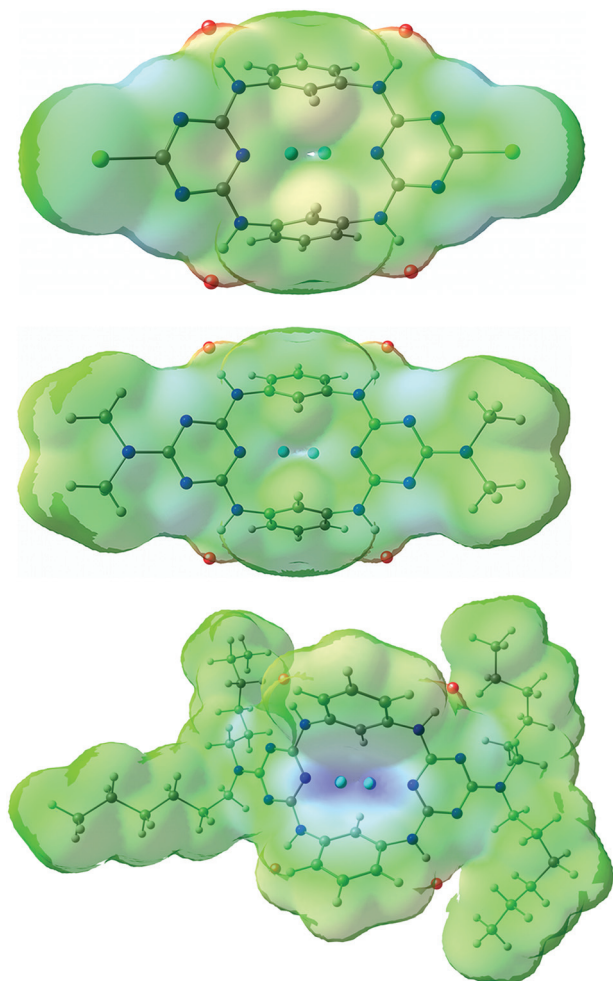


Fig. 1 Electrostatic potential mapped on the molecular electron density surface (0.001 electrons bohr⁻³) for **10** (top), **11** (middle) and **12** (bottom). The colour scale ranges from blue (-50.8 kcal mol⁻¹) to red (44.0 kcal mol⁻¹). The red and cyan dots correspond to the location of $V_{s,max}$ and $V_{s,min}$ values respectively.

the base-catalyzed nucleophilic substitution of the hydrogen nitrogen bridging atoms by four methyl ester pendant arms. The $V_{s,max}$ and $V_{s,min}$ values were calculated at HF/6-311+G** from the structures of **10–12** previously optimized at the same level of theory with Gaussian 09²³ and are gathered in Table 1.

The three macrocycles exhibit four well-defined positive regions drawn in red on the electrostatic potentials mapped on the electron densities of **10–12**, shown in Fig. 1 with maxima depicted as red dots positioned at short distances from the hydrogen atoms of the nitrogen bridges (*ca.* 1.21 Å). Furthermore, the four $V_{s,max}$ values for **10** are higher than for **11** and **12**, indicating that the former macrocycle is more acidic on the nitrogen bridges due to the electron withdrawing promoted by both chlorine-substituted triazine rings. In agreement, the macrocycle **10** has a negative region located inside the macrocyclic cavity with two close $V_{s,min}$ values of only -35.5 and -35.4 kcal mol⁻¹ and depicted by the two cyan dots in Fig. 1 (top). In contrast, the dialkylamine substituents on both triazine rings make the calix framework electron rich and consequently the two minima shown in Fig. 1 for **11** (middle) and **12** (bottom) are more negative than for **10** (see Table 1). In other words, **11** and **12** are more basic in the centre of the macrocyclic cavity and less acidic on the four N–H bridging groups.

This analysis is entirely consistent with the experimental reactivity observed for **10–12**. In macrocycle **10**, with higher $V_{s,max}$ values, the hydrogen N-bridging atoms are more easily released than in **11** and **12**, and consequently, **10** is more reactive towards base-catalysed nucleophilic substitution. By contrast, the macrocycles **11** and **12** with similar local maxima potentials have similar acidities, hence identical nucleophilic reactivities are expected. Therefore, the non-reactivity of **11** seems to be dictated by its poor solubility in acetonitrile.

Single crystal X-ray structures of **1**, **2** and **12**

The structure of the association between **1** and dimethyl diglycolate with a stoichiometry 1 : 1 observed in the solid state is presented in Fig. 2. This association has a 2-fold crystallographic axis running through the oxygen atom of the ether diglycolate linkage. The macrocycle exhibits the usual 1,3-alternate conformation²⁴ with four methyl acetate arms located

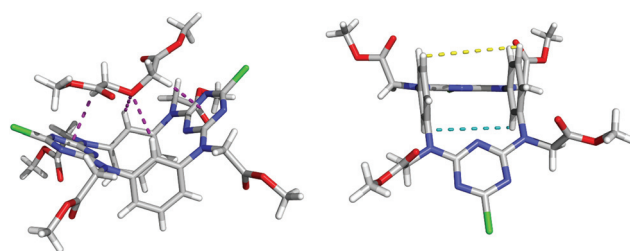


Fig. 2 Association between **1** and dimethyl diglycolate in solid state is shown in the left plot with the neutral substrate through the C–H...O hydrogen bonds and C–H... π interactions, which are drawn as purple dashed lines. The plot at the right emphasizes the almost parallel disposition of the two phenyl rings in 1,3-alternate conformation together with $H_{ortho}\cdots H_{ortho}$ and $H_{meta}\cdots H_{meta}$ distances drawn as yellow and cyan teal dashed lines, respectively.

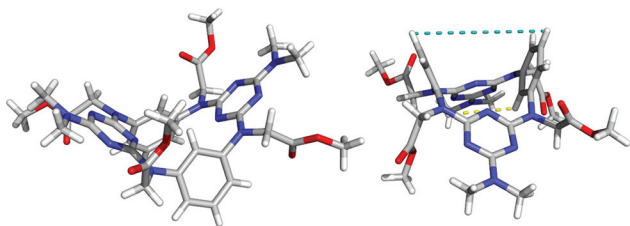


Fig. 3 Molecular structure of **2** illustrating the spatial disposition of the four methyl ester pendant arms relative to the N_4 bridge plane (left) and the nonparallel disposition of two phenyl rings relative to each other (right). Remaining details as given in Fig. 2.

below the macrocyclic plane defined by the four nitrogen bridges, henceforth denominated as the N_4 bridging plane. The substrate is positioned over the narrow rim of azacalix[2]-arene[2]triazine with C–H...O distances between two *ortho*-hydrogen atoms of both phenyl rings and the ether oxygen atom of dimethyl diglycolate of 2.80 Å. Furthermore, one hydrogen of each methylene group points to an electron deficient triazine ring at a C–H centroid ring distance of 2.87 Å. These distances, drawn in Fig. 2 (left plot) as purple dashed lines, seem to indicate that the association is stabilized by weak C–H...O hydrogen bonds and C–H... π interactions, apart from the other electrostatic interactions derived from crystal packing.

The asymmetric unit of **2** consists of one macrocycle, shown in Fig. 3, and one THF solvent crystallization molecule. As observed for **1**, the macrocycle **2** exhibits a 1,3-alternate conformation, but with tetramethyl ester pendant arms showing a different spatial disposition. In **2**, a carboxylate methoxy group located above (+) the N_4 plane is followed by another positioned below this plane (–), leading to a conformation type +– (Fig. 3, right), whereas in **1**, as a consequence of the dimethyl diglycolate position, the conformation adopted is –– (Fig. 2, left).

It is noteworthy that the two 1,3-alternate conformations of these two macrocycles correspond to different shapes, as is evident from the structural comparison presented in ESI (Table S1†). Indeed, the two phenyl rings in **1** are almost parallel (see Fig. 2, right) with distances between the *ortho* (the hydrogen atoms between the nitrogen bridges, $H_{ortho}\cdots H_{ortho}$) and *meta* hydrogen atoms ($H_{meta}\cdots H_{meta}$) of 4.49 and 4.80 Å, respectively. In contrast in **2**, the $H_{ortho}\cdots H_{ortho}$ distances of 3.70 Å are markedly shorter than the $H_{meta}\cdots H_{meta}$ distances of 6.77 Å showing the existence of a wider rim. Furthermore, in **2** the phenyl rings intercept the N_4 plane at dihedral angles (Ω) of 68.3 and 71.4°, while in **1** the phenyl rings are roughly perpendicular to this plane with Ω angles of 88.4°. In contrast, in both compounds, the triazine rings are tilted relatively to the N_4 plane by comparable dihedral angles (ϕ) of 33.7° for **1** and 35.2 and 36.0° for **2**.

The asymmetric unit of **12** is composed of three discrete molecules, one of macrocycle and two $CHCl_3$ solvent crystallization molecules as shown in Fig. 4. It is noteworthy that the macrocycle exhibits an unprecedented conformation for

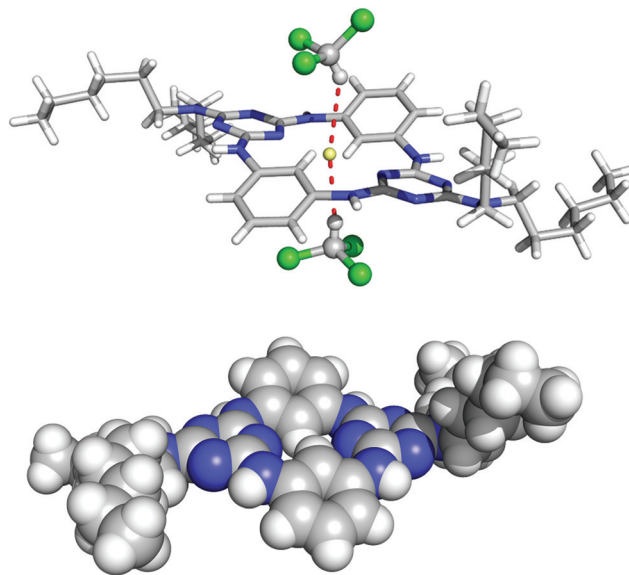


Fig. 4 Different structural features of the solid state structure of **12**: molecular diagram in the top shows the two $CHCl_3$ solvent molecules positioned above and below the macrocycle with C–H groups at distances from the plane defined by the azacalix[2]arene[2]triazine scaffold consistent with the existence of C–H... π interactions, which are depicted as red dashed lines (the yellow dot is the centroid defined by the nitrogen bridging atoms); view in the bottom shows **12** in space filling model emphasizing the ladder type conformation and the short distance between *ortho* phenyl protons.

azacalix[2]arene[2]triazine derivatives (as revealed by a search on CSD)²⁴ with the two phenyl rings adopting an almost anti-parallel disposition with a dihedral angle of 2.5°. The two *ortho* hydrogen atoms are facing each other, giving a shorter $H_{ortho}\cdots H_{ortho}$ distance of 2.75 Å when compared with the corresponding distances in **1** (4.49 Å) and **2** (3.70 Å). The triazine rings are nearly coplanar with the N_4 bridging plane consistent with ϕ angles of 2.8 and 4.3°, whereas the phenyl rings intercept this plane at a Ω angle of 25.8 and 28.2° leading to a ladder type conformational shape, as depicted in the perspective view presented in Fig. 4 (bottom). An unusual flattened partial cone conformation was also observed for the related tetraoxacalix[2]arene[2]triazine derivative bearing benzyloxy and methyl ester substituents on both benzene rings, while for an analogous macrocycle, in which these bulky groups are replaced by *tert*-butyl groups, this conformation coexists in the solid state, as a major component, with the common 1,3-alternate conformation.²⁵ In contrast to **12**, in these molecules the phenyl rings adopt a spatial disposition roughly perpendicular to the O_4 bridging plane with Ω angles of 86.0 and 85.1° for the former and second macrocycle, respectively.

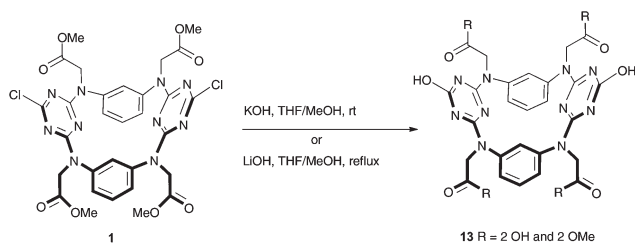
Another intriguing structural feature in **12** is the location of the two crystallographically independent solvent molecules above and below the macrocycle, with the corresponding C–H groups at distances of 2.19 and 2.57 Å from the N_4 bridging plane. These distances suggest the existence of C–H... π interactions between the acidic C–H chloroform groups and π electron azacalix[2]arene[2]triazine rich system promoted by the

N-dihexylamine substituents on triazine rings and the almost flattened conformation. Indeed, the ladder type conformation is converted into the 1,3-alternate one when **12** is optimised in the gas-phase at the HF/6-311+G** level of theory. Therefore, the ladder conformation type observed in the crystal structure is governed by a delicate balance between the electronic nature of azacalix[2]arene[2]triazine scaffold and packing effects.

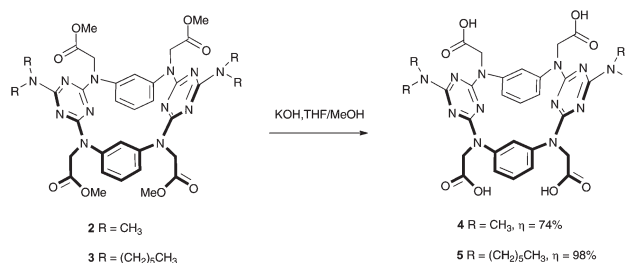
The N–C bridges distances have comparable values in the three macrocycles following the usual pattern exhibited by azacalix[2]arene[2]triazine, *i.e.* the distances to triazine rings are shorter than those to phenyl rings in agreement with a double sp^2/sp^3 hybridization state for nitrogen bridging atoms (Table S1†). Nevertheless, the distances of a second set in **12** are systematically 0.02 Å shorter than the corresponding ones in **1** and **2**, indicating a more efficient electron delocalization through the azacalix[2]arene[2]triazine scaffold in **12**, in agreement with the different conformational shape adopted by this macrocycle when compared with **1** and **2**.

Hydrolysis of the *N*-tetramethyl ester pendant arms

In order to obtain suitable ligands for metal coordination the hydrolysis of the methyl ester pendant arms was carried out using either basic or acidic conditions. Firstly, the saponification of **1** was performed in THF–MeOH (1 : 1) solvent system using KOH or LiOH aqueous solutions as strong bases. In both reaction conditions, a mixture of three possible isomeric compounds **13**, bearing two carboxylic groups and two methyl ester groups, adjacent to the phenyl or triazine rings or in alternate positions, was obtained (Scheme 4) in *ca.* 62% yield after acidification of the reaction mixture with HCl (6 N) at pH = 1. The substitution of the chlorine atoms of both triazine moieties by hydroxyl groups was also observed. The presence of two methyl ester groups was confirmed in the ^1H NMR spectrum with the singlet at δ 3.82 ppm integrating to six protons of two methoxy groups. The ^{13}C NMR spectrum showed two resonances at δ 170.5 and 171.3 ppm, indistinguishably assigned to the ester and acid carbonyl groups. Further experimental evidence for the partial hydrolysis of the methyl ester groups was acquired through the negative ion ESI-MS technique with the appearance of the $[\text{M} - \text{H}]^-$ ion peak at m/z 661 and $[\text{M} + \text{Na} - 2\text{H}]^-$ adduct at m/z 683 in agreement with the existence of a mixture of isomeric compounds **13** having two carboxyl and two methyl ester pendant arms. The replacement of chlorine atoms by two hydroxyl groups was



Scheme 4 Hydrolysis of *N*-methyl ester appendages of **1** in basic conditions.



Scheme 5 Tetra-carboxylic acids derivatives **4** and **5** obtained respectively from **2** and **3** azacalix[2]arene[2]triazine methyl ester analogues.

confirmed by the absence of the isotopic $[\text{M} + 2]^+$ and $[\text{M} + 4]^+$ ion peaks in the positive ion mode ESI-MS spectrum.

Subsequently, the hydrolysis of **1** was also undertaken in acidic medium of HCl (6 or 10 N). Under these reaction conditions a water-soluble product was obtained, suggesting the formation of the tetra-carboxylic acid. Unfortunately, all attempts to isolate this compound were unsuccessful, even as a hydrochloric salt.

In contrast to what happened with **1**, all four methyl ester groups of **2** and **3** were hydrolyzed with KOH in the THF–MeOH solvent mixture leading to the target compounds **4** and **5**, which were obtained in good yields of 74% and 98%, respectively (Scheme 5), after acidification. The formation of these two macrocycles was attested by the absence of the methyl ester protons from the corresponding precursors in their ^1H NMR spectra. In agreement, the ESI-MS spectra carried out in negative ion mode showed $[\text{M} - \text{H}]^-$ and $[\text{M} + \text{Na} - 2\text{H}]^-$ peaks at m/z 687 and 709 for **4** respectively, and 968 and 990 for **5** in the same order.

Coordination studies

The coordination ability of the macrocycles **4** and **5** for transition metals was investigated with copper(II) through the UV-vis spectroscopy. The four carboxylic groups of both macrocycles can be deprotonated depending on the medium pH. Therefore, in order to avoid the formation of species with different protonation states only the fully protonated (acid) and the fully deprotonated (basic) forms of both were evaluated. In addition, due to solubility reasons, the acid form was investigated in dry methanol and the basic form in water at pH \approx 11. The spectra of the macrocycles and their metal complexes were recorded and are presented in ESI as Fig. S43–S46.† The corresponding UV-vis absorption bands are summarized in Table 2.

In both solvents the UV-vis spectra of free ligands **4** and **5** display absorption bands typical of ILCT transitions. Furthermore when a CuCl_2 solution is added to solutions of **4** and **5**, new absorption bands appear in the spectra, which correspond to the ligand field d–d and LMCT transitions. The d–d bands have very low intensities when compared with the remaining ones. The ILCT bands do not suffer a substantial wavelength shift with the coordination of Cu^{2+} to both macrocycles.

The stoichiometry of the complexes formed between the Cu^{2+} and the macrocycles **4** and **5**, in the acid form, was

Table 2 UV-vis absorption bands for the d-d, LMCT and ILCT transitions of **4** and **5** and their copper(II) complexes with λ_{\max} in nm

Species	Solvent	d-d	LMCT	ILCT
4	H ₂ O	—	—	351
	CH ₃ OH	—	—	237.2, 242.8, 249.2, 255.4, 261.5, 268.3, 272 (sh) ^b
4 ·Cu ²⁺	H ₂ O	nd ^a	421	351
	CH ₃ OH	675	341.5	238.2, 243.2, 249.2, 255.4, 261.5, 268.3, 272 (sh) ^b
5	H ₂ O	—	—	242.5
	CH ₃ OH	—	—	238.2, 246.3, 252.0, 259.6, 266.5, 272 (sh) ^b
5 ·Cu ²⁺	H ₂ O	636	336.1	242.5
	CH ₃ OH	654	371.5	238.2, 246.3, 252, 259.6, 266.5, 272 (sh) ^b

^aThe band was not observed by solubility reasons. ^bsh means shoulder.

determined using the mole ratio method in methanol at 20 °C. The addition of increasing amounts of Cu²⁺ to the solution of **4** or **5** leads to an intensity decrease of the absorption bands between 260 and 270 nm till 1 equivalent of metal is added as shown in Fig. 5. From this stage, no change in the absorbance was observed, which indicates a 1:1 metal:ligand stoichiometry (Fig. 5). Moreover, a band at *ca.* 300–400 nm, attributed to the LMCT as earlier described, is present throughout the titrations. The stability constants of Cu²⁺ complexes were determined from the titration data using the HypSpec software²⁶ and log *K* values of 6.70 ± 0.2 for **4** and 6.65 ± 0.2 for **5** were estimated. These values indicate that both macrocycles are able to coordinate the metal centre with equivalent strengths, thus affording complexes with coordination spheres

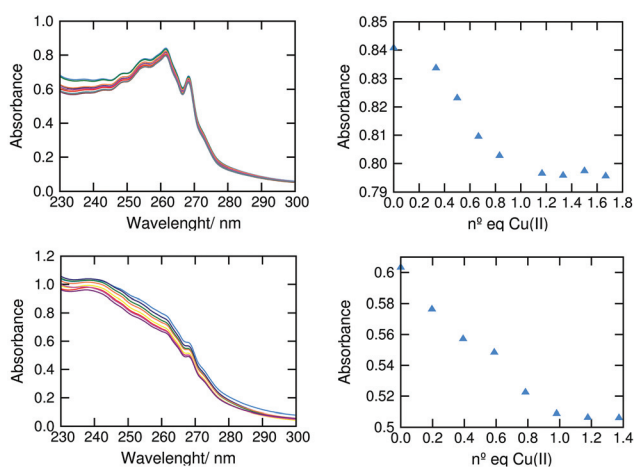


Fig. 5 Titration of **4** and **5** in dry methanol with CuCl₂ by means of UV spectroscopy: UV-vis spectra of **4** (7.96×10^{-6} M – top left) and **5** (1.35×10^{-5} M – bottom left) recorded at 20 °C by the addition of increasing amount of CuCl₂; absorbance variation versus Cu²⁺ equivalents added at λ_{\max} 261.5 nm for **4** (top right) and at λ_{\max} 266.5 nm for **5** (bottom right).

eventually composed of nitrogen bridging atoms and carboxylate oxygen donor atoms. Unfortunately the Cu²⁺ complexes of **4** and **5** did not afford suitable crystals for single crystal X-ray diffraction determination, and further coordination studies on these complexes are beyond of the scope of this work. To the best of our knowledge, and in contrast with tetra-oxacalix[2]arene[2]triazine derivatives,¹⁷ this preliminary coordination study is the first one reported on azacalix[2]arene[2]triazine based artificial receptors.

Equivalent titration studies with both macrocycles, in their basic forms, were not possible to be undertaken due to the formation of precipitated hydroxo complexes in the presence of high amounts of metal.

Conclusions

Two synthetic approaches to afford azacalix[2]arene[2]triazine macrocycles armed on the nitrogen bridges with four methyl ester groups were explored. However, our studies showed that the macrocycle **1** is only successfully obtained from the undecorated azacalix[2]arene[2]triazine **10** platform, after the macrocyclization process. Afterwards, **1** can be straightforwardly used to prepare the macrocycles **2** and **3** by the single S_NAr replacement of the chlorine atoms by dimethylamine and dihexylamine respectively. Otherwise, these two macrocycles can be obtained from the corresponding dialkyl azacalix[2]arene[2]triazine intermediates **11** and **12**, but this synthetic pathway is less efficient. The four N–H bridged atoms in **11** and **12** are less acidic than in **10** and, in agreement with the computed *V*_{s,max} values, the nitrogen bridges of **11** and **12** are less reactive to the base catalyzed nucleophilic substitution.

The hydrolysis of all four *N*-methyl ester pendant arms was only successfully achieved when strong basic conditions were used to afford the target macrocycles **4** and **5** from **2** and **3** respectively. In contrast, in **1**, the two chlorinated triazine ring positions are still reactive, and then, concomitantly with the random hydrolysis of two methyl ester groups, the nucleophilic substitution of both triazine chlorine atoms by hydroxyl groups occurs.

The preliminary coordination studies showed that the macrocycles **4** and **5** are able to form Cu²⁺ complexes under either basic or acidic conditions. The search for neutral receptors based on the azacalix[2]arene[2]triazine platform able to recognise cations and anions continues to progress at our laboratories.

Experimental section

General remarks

All reagents were used as supplied without further purification. All solvents were purified and dried before use according to standard methods.²⁷ Melting points were determined with a Reicher Model Thermovar melting-point apparatus without further correction. LRMS spectra were obtained on a

Bruker Daltonic Esquire 3000 Ion Trap Mass Spectrometer with ESI-ITD-MS/MS positive or negative ion mode while HRMS (ESI) measurements were performed on a Bruker Daltonics ApexQe FTICR Mass Spectrometer equipped with a combined Apollo II electrospray/MALDI ion source and a 7 T actively shielded superconducting magnet. ^1H , ^{13}C (APT) and ^2D NMR (HMQC and COSY) spectra were recorded on a Bruker CXP400 spectrometer operating at 400 MHz using one of the following deuterated solvents: DMSO- d_6 (99.9%), acetone- d_6 or CDCl_3 . All chemical shifts are given in ppm and using tetramethylsilane as an internal reference. UV-vis spectra were recorded with a Shimadzu UV-2450 spectrophotometer.

N,N'-Bis(dichloro-*s*-triazinyl)-*m*-phenylenediamine, **7**, was prepared as previously described by Wang *et al.*¹⁴

Azacalix[2]arene[2]triazine, 10. As mentioned above this macrocycle was obtained using an experimental procedure slightly different from that previously reported by Wang *et al.*¹⁴ The diamine **6** (1.11 mmol, 0.12 g) and the trimer **7** (1.11 mmol, 0.45 g), previously dissolved in acetone (98 mL), were simultaneously added dropwise at the same rate to a solution of diisopropylethylamine (0.46 mL, 2.75 mmol) in acetone (224 mL) at 65 °C for 8 h. The reaction mixture was stirred under nitrogen at room temperature for the subsequent 7 days leading to a white precipitate, which was filtered and washed with water and then with acetone. The intermediate macrocycle **10** was obtained (278 mg, 57%) as a white solid, m.p. >350 °C; ^1H NMR (400 MHz, DMSO- d_6 , 25 °C): δ = 10.00 (s, 4H), 7.75 (s, 2H), 7.22 (t, J = 7.9 Hz, 2H), 6.79 (d, J = 7.5 Hz, 4H) ppm; ^{13}C NMR (101 MHz, DMSO- d_6 , 25 °C): δ = 168.0, 164.3, 137.9, 128.9, 118.8, 118.1 ppm.

***N,N,N,N*-Tetracarboxymethylazacalix[2]arene[2]triazine, 1.** Methyl bromoacetate (3.28 mmol, 0.3 mL) was added to a dispersion of **10** (0.41 mmol, 0.18 g) in CH_3CN (3.5 mL) containing Cs_2CO_3 (4.1 mmol, 1.34 g). The reaction was carried out at 65 °C under stirring for 3 h. Subsequently, CHCl_3 was added to the reaction crude and the organic phase was successively washed with an aqueous solution of HCl 10%, and a solution of NaHCO_3 and brine. The organic phase was dried with magnesium sulfate and concentrated under vacuum. The macrocycle **1** was purified by flash chromatography using as an eluent cyclohexane–acetone (3 : 2). A white solid was obtained (180 mg, 59% yield), m.p. 170–172 °C; IR (KBr) ν_{max} 1749 (C=O ester), 1568, 1498, 1473 (CC Ar), 1200 (C–O ester), 802 (C–Cl) cm^{-1} ; ^1H NMR (400 MHz, CDCl_3 , 25 °C): δ = 7.20–7.14 (m, 2H), 7.04 (s, 4H), 7.02–7.01 (m, 2H), 4.47 (s, 8H), 3.75 (s, 12H) ppm; ^{13}C NMR (101 MHz, CDCl_3 , 25 °C): δ = 169.7, 169.4, 165.7, 143.4, 130.0, 129.1, 127.4, 52.3, 51.5 ppm; ESI-MS m/z 749 $[\text{M} + \text{Na}]^+$; 731 $[\text{M} + \text{H} + 4]^+$; 729 $[\text{M} + \text{H} + 2]^+$; 727 $[\text{M} + \text{H}]^+$; MS^2 $(\text{M} + \text{H})^+$ m/z 695 $[\text{M} + \text{H} - \text{CH}_3\text{OH}]^+$; 667 $[\text{M} + \text{H} - \text{C}(\text{OH})\text{OCH}_3]^+$; 631 $[\text{M} + \text{H} - (\text{C}(\text{OH})\text{OCH}_3 + \text{HCl})]$; 607 $[\text{M} + \text{H} - 2 \times \text{C}(\text{OH})\text{OCH}_3]^+$; HRMS (ESI) calcd for $\text{C}_{30}\text{H}_{29}\text{Cl}_2\text{N}_{10}\text{O}_8^+$ $[\text{M} + \text{H}]^+$: 727.1469, found 727.1510.

General procedure for the synthesis of **11** and **12**

To a solution of **10** (0.46 mmol, 0.2 g) and K_2CO_3 (1.24 mmol, 0.171 g) in DMF (14 mL) was added a dialkylamine

(0.97 mmol). The mixture was stirred for 24 h at 70 °C. Afterwards, ethyl ether was added to the crude reaction and the resulting organic phase was washed with water. The organic phase was evaporated under reduced pressure to give the required macrocycle.

Di(dimethylamino)azacalix[2]arene[2]triazine, 11. A general reaction of **10** with dimethylamine gave **11** (107 mg, 51% yield), m.p. > 350 °C; ^1H NMR (400 MHz, DMSO- d_6 , 25 °C): δ = 8.77 (s, 4H, NH), 7.80 (s, 2H), 7.09 (t, J = 7.9 Hz, 2H), 6.76–6.60 (m, 4H), 3.10 (s, 12H) ppm; ^{13}C NMR (101 MHz, DMSO- d_6 , 25 °C): δ = 165.0, 164.6, 139.6, 128.2, 116.4, 116.3, 35.5 ppm; ESI-MS m/z 479 $[\text{M} + \text{Na}]^+$; 457 $[\text{M} + \text{H}]^+$; MS^2 $(\text{M} + \text{H})^+$ m/z 412 $[\text{M} + \text{H} - \text{HN}(\text{CH}_3)_2]^+$, 387.

Di(dihexylamino)azacalix[2]arene[2]triazine, 12. A general reaction of **10** with dihexylamine afforded **12** as a white solid (258 mg, 76% yield), m.p. > 350 °C; ^1H NMR (400 MHz, CDCl_3 , 25 °C): δ 8.24 (s, 2H), 7.03 (t, 2H, J = 7.70 Hz), 6.45 (br, s, 4H), 6.67 (s, 4H), 3.40 (t, 8H, J = 6.75 Hz), 1.58–1.52 (m, 8H), 1.25 (s, 24H), 0.83 (t, J = 6.75 Hz, 12H) ppm; ^{13}C NMR (101 MHz, CDCl_3 , 25 °C): δ 164.9, 146.0, 128.9, 115.3, 110.7, 46.4, 31.7, 27.9, 26.7, 22.7, 14.1 ppm; TOF-MS m/z 737 $[\text{M} + \text{H}]^+$; 369 $[\text{M} + \text{H} - 2 \times \text{HN}(\text{CH}_2)_5\text{CH}_3]^+$.

Di(dimethylamino)-*N,N,N,N*-tetracarboxymethylazacalix[2]arene[2]triazine 2. A reaction of **1** (0.46 mmol) with dimethylamine (0.97 mmol) following the general procedure earlier described to prepare **11** and **12**, afforded **2** (281 mg; 82%) as a white solid, m.p. 206–209 °C, after purification through the flash chromatography using 3 : 1 cyclohexane–acetone as an eluent. IR (KBr) ν_{max} 2935 (C–H), 1751 (C=O ester), 1541, 1458 (CC Ar), 1203 (C–N), 1198 (C–O ester) cm^{-1} ; ^1H NMR (400 MHz, CDCl_3 , 25 °C): δ 7.16–7.10 (m, 4H), 7.00 (dd, J = 7.9, 1.6 Hz, 4H), 4.39–4.28 (m, 8H), 3.71 (s, 12H), 3.05 (s, 12H) ppm; ^{13}C NMR (101 MHz, CDCl_3 , 25 °C): δ 171.3, 165.5, 165.1, 144.5, 130.7, 129.3, 126.0, 52.7, 51.8, 35.8 ppm; ESI-MS m/z 767 $[\text{M} + \text{Na}]^+$; 745 $[\text{M} + \text{H}]^+$; MS^2 $(\text{M} + \text{H})^+$ m/z 685 $[\text{M} + \text{H} - \text{CH}_3\text{OCOH}]^+$; 625 $[\text{M} + \text{H} - 2 \times \text{CH}_3\text{OCOH}]^+$; 565 $[\text{M} + \text{H} - 3 \times \text{CH}_3\text{OCOH}]^+$.

Di(dihexylamino)-*N,N,N,N*-tetracarboxymethyl azacalix[2]arene[2]triazine, 3. The macrocycle was prepared following two alternative synthetic pathways as described above. In the route depicted in Scheme 3, the macrocycle **3** was produced by the reaction of **1** with dihexylamine, (0.97 mmol) using the general procedure described above to synthesize **11** and **12**. The flash chromatography of crude reaction using as an eluent cyclohexane–acetone (3 : 1) provided the macrocycle **3** (240 mg, 51%) as a white solid, m.p. 150–153 °C; IR (KBr) ν_{max} 2937 (C–H), 2918 (C–H), 2850 (C–H), 1736 (C=O ester), 1541, 1458 (CC Ar), 1199 (C–N), 1194 (C–O ester) cm^{-1} ; ^1H NMR (400 MHz, CDCl_3 , 25 °C): δ = 7.15–7.10 (m, 4H), 6.99 (dd, J = 7.8, 1.6 Hz, 4H), 4.35 (q, J = 17.1 Hz, 8H), 3.69 (s, 12H), 3.40 (tt, J = 17.0, 8.5 Hz, 8H), 1.60–1.47 (m, 8H), 1.36–1.28 (m, 24H), 0.91 (t, J = 6.7 Hz, 12H) ppm; ^{13}C NMR (101 MHz, CDCl_3 , 25 °C): δ = 171.2, 165.6, 164.4, 144.6, 130.9, 129.2, 126.2, 52.4, 51.7, 47.4, 31.9, 28.1, 26.8, 22.8, 14.1 ppm; ESI-MS m/z 1048 $[\text{M} + \text{Na}]^+$; 1025 $[\text{M} + \text{H}]^+$; MS^2 $(\text{M} + \text{H})^+$ m/z 965 $[\text{M} + \text{H} - \text{CH}_3\text{OCOH}]^+$; 905 $[\text{M} + \text{H} - 2 \times \text{CH}_3\text{OCOH}]^+$.

Compound **3** was also prepared by the synthetic route described in Scheme 2 as follows: to a dispersion of **12** (0.41 mmol, 0.302 g) in CH₃CN (3.5 mL) having Cs₂CO₃ (6.56 mmol, 2.14 g) was added methyl bromoacetate (6.56 mmol, 0.6 mL). The reaction mixture was stirred at 50 °C for 3 h. The macrocycle **3** was obtained (176 mg, 42% yield) after work-up as described above for **1**.

General procedure for the hydrolysis of the *N*-tetramethyl ester macrocycles

To a solution of **1**, **2** or **3** (0.146 mmol) in THF–MeOH (1.42 mL/1.42 mL) an aqueous solution of KOH (5.40 mmol, 0.302 g) in 0.46 mL of water was added. The mixture was stirred for 24 h at room temperature and the solvents were removed under vacuum. The crude reaction was dissolved in water (3.6 mL) and the acidification of the solution to pH 1 with 10% HCl triggered the precipitation of the macrocycle requested.

Dihydroxy-*N,N*-dicarboxymethyl-*N,N*-dicarboxylazacalix[2]arene[2]triazine, **13.** A mixture of isomeric macrocycles having two carboxylic and two methyl esters was obtained from **1** using the general hydrolysis procedure as a white solid (60 mg, yield of 62%); IR (KBr) ν_{\max} 1701 (C=O acid), 1578, 1527 (CC Ar), 1367 (C–N), 1207 (C–O acid) cm⁻¹; ¹H NMR (400 MHz, DMSO-*d*₆, 25 °C): δ = 12.71 (s, 2H), 7.25 (t, *J* = 7.9 Hz, 2H), 7.03 (dd, *J* = 10.0, 2.1 Hz, 6H), 4.31 (dd, *J* = 34.6, 17.6 Hz, 8H), 3.82 (s, 6H) ppm; ¹³C NMR (101 MHz, DMSO-*d*₆, 25 °C): δ = 171.3, 170.5, 166.7, 144.1, 130.2, 129.7, 126.3, 54.1, 52.6 ppm. ESI-MS *m/z* 683 [M + Na – 2H]⁻; 661 [M – H]⁻; MS² (M – H)⁻ *m/z* 617 [M – H – CO₂]⁻; 573 [M – H – (COHOHCH₂ + CO)]⁻; 529 [M – H – (COHOHCH₂ + CO + CO₂)]⁻; 485 [M – H – 2 × (COHOCH₃ + CO)]⁻.

Di(dimethylamino)-*N,N,N,N*-tetracarboxymethylazacalix[2]arene[2]triazine, **4,** was straightforwardly prepared through the general procedure of hydrolysis from **2** as a white solid (109 mg; 74% yield), m.p. 278–281 °C; IR (KBr) ν_{\max} 2922 (O–H), 1707 (C=O acid), 1587, 1545 (CC Ar), 1245 (C–N), 1203 (C–N) cm⁻¹; ¹H NMR (400 MHz, DMSO-*d*₆, 25 °C): δ = 7.21–7.02 (m, 8H), 4.54–4.24 (m, 8H), 3.05 (s, 12H) ppm; ¹³C NMR (101 MHz, DMSO-*d*₆, 25 °C): δ = 171.7, 166.5, 165.2, 145.7, 131.6, 130.0, 126.5, 53.0, 35.8 ppm. ESI-MS *m/z* 709 [M + Na – 2H]⁻; 687 [M – H]⁻; MS² (M – H)⁻ *m/z* 643 [M – H – N(CH₃)₂]⁻; 599 [M – H – (COHOHCH₂ + CO)]⁻; 555 [M – H – (COHOHCH₂ + CO + CO₂)]⁻; 511 [M – H – 2 × (COHOCH₃ + CO)]⁻; HRMS (ESI) calcd for C₃₀H₃₃N₁₂O₈⁺ [M + H]⁺: 689.2466, found 689.2517; elemental analysis calcd (%) for C₃₀H₃₂N₁₂O₈·3H₂O: C 48.52, H 5.16, N 22.63; found: C 48.87, H 5.10, N 23.00.

Di(dihexylamino)-*N,N,N,N*-tetracarboxymethylazacalix[2]arene[2]triazine, **5.** This macrocycle was obtained from **3** by the general hydrolysis procedure. After acidification with HCl, the crude reaction was extracted with dichloromethane. Subsequently, this organic phase was dried with magnesium sulfate, filtered and concentrated under vacuum. The macrocycle **5** was provided (99 mg; 98% yield) as a white solid, m.p. 257–258 °C; IR (KBr) ν_{\max} 2922 (O–H), 1716 (C=O acid), 1541, 1458 (CC Ar), 1238 (C–N), 1201 (C–N) cm⁻¹; ¹H NMR

(400 MHz, acetone-*d*₆, 25 °C): δ = 7.21–7.02 (m, 8H), 4.54–4.24 (m, 8H), 3.58–3.44 (m, 8H), 1.63 (s, 8H), 1.40–1.24 (m, 24H), 0.89 (t, *J* = 6.4 Hz, 12H) ppm; ¹³C NMR (101 MHz, acetone-*d*₆, 25 °C): δ = 171.7, 166.5, 165.2, 145.7, 131.6, 130.0, 126.5, 53.0, 48.1, 32.5, 27.6, 23.4, 14.4 ppm; ESI-MS *m/z* 990 [M + Na – 2H]⁻; 968 [M – H]⁻; MS² (M – H)⁻ *m/z* 924 [M – H – CO₂]⁻; 880 [M – H – (COHOHCH₂ + CO)]⁻; 836 [M – H – (COHOHCH₂ + CO + CO₂)]⁻; 792 [M – H – 2 × (COHOCH₃ + CO)]⁻; HRMS (ESI) calcd for C₅₀H₇₃N₁₂O₈⁺ [M + H]⁺: 969.5596, found 969.5652; elemental analysis calcd (%) for C₅₀H₇₂N₁₂O₈·2H₂O·CH₃OH: C 59.05, H 7.77, N 16.20; found: C 59.42, H 7.53, N 15.82.

UV-vis spectrophotometric measurements

The metal complexes in water were prepared by addition of copper(II) chloride salt (0.4 eq.) to a solution of **4** or **5** (1.38 × 10⁻³ or 3.09 × 10⁻³ M). The pH was maintained around 11 using a standard solution of KOH. The lower concentration solutions allowed the measurement of the absorption bands in the ultraviolet region, while for more concentrated solutions the absorption bands were measured in the visible region.

Titration curves were performed by addition of small amounts of the chloride copper(II) salt to **4** and **5** in their acid forms in a dry methanol solution at 293.2 ± 0.1 K. The copper(II) salt in dry methanol solution was standardized as described in ref. 28. The concentration of each macrocycle was determined by the method of continuous variation.²⁹

The stability constants of **4** and **5** Cu²⁺ complexes were calculated by fitting the corresponding spectrophotometric titration data with the HypSpec program.²⁶ The molar absorbance of free macrocycles in methanol and in water solutions was measured in a separate experiment and kept constant for all subsequent determinations. The errors quoted are the standard deviations of the overall stability constants given directly by the program for the input data, which include all the experimental points from all titration curves.

X-ray crystallography

Single crystal X-ray diffraction data for **1**, **2** and **12** were collected on a Bruker SMART APEX II diffractometer with a CCD area detector using graphite monochromatized Mo-K α radiation (λ = 0.71073 Å) at 150(2) K. The frames were integrated with the SAINT-Plus software package,³⁰ and the intensities were corrected for polarization and Lorentz effects. Absorption corrections for all data sets were applied *via* the multi-scan procedure using the SADABS³¹ from the same graphical suite. The structures were solved by a combination of direct methods with subsequent difference Fourier syntheses and refined by full matrix least squares on *F*² using the SHELX-97 suite,³² and final refinements were carried out with SHELXL-2013.³² Anisotropic thermal displacements were used for all non-hydrogen atoms. The hydrogen atoms were inserted at geometrical positions with *U*_{iso} = 1.2 *U*_{eq} to those to which they are attached. Crystal data and refinement details for the three macrocycles are summarized in Table S2 given in the ESI.† Molecular diagrams were drawn with Pymol.³³ Crystal data for the structures have been deposited with the Cambridge

Crystallographic Data Centre, CCDC: 957200, 1, 957201, 2, and 957202, 12.

Quantum calculations

The structures of 10–12 were fully optimised at the HF/6-311+G** level of theory without any symmetry constraints using the Gaussian09.²³ Afterwards, the electrostatic potential and the wave functions for these molecules were generated by single-point calculations following the methodology described by Politzer *et al.*³⁴ Accordingly, the electrostatic potential was evaluated on the 0.001 electron per bohr³ contour of the electron density surface and the surface-electrostatic potential maxima points ($V_{S,max}$) were computed using the Wavefunction Analysis Program gently provided by Bulat.³⁵

Acknowledgements

The authors are grateful for funding from QREN-FEDER, through the Operational Program Competitiveness Factors – COMPETE, and National Funds through the FCT under project PTDC/QUI-QUI/101022/2008 and Pest-OE/QUI/UI0612/2013. J.M.C. and S.C. thank FCT for PhD scholarship SFRH/BD/66789/2009 and postdoctoral grant SFRH/BPD/42357/2007 respectively. We also acknowledge Paula Branco from ASAE for the mass spectra.

Notes and references

- (a) G. Blotny, *Tetrahedron*, 2006, **62**, 9507–9522; (b) M. Vidal-Mosquera, A. Fernández-Carvajal, A. Moure, P. Valente, R. Planells-Cases, J. M. González-Ros, J. Bujons, A. Ferrer-Montiel and A. Messegueur, *J. Med. Chem.*, 2011, **54**, 7441–7452; (c) K. Xie, A. Hou and X. Wang, *Carbohydr. Polym.*, 2008, **72**, 646–651; (d) G. Müller, *History of the Discovery and Development of Triazine Herbicides in The Triazine Herbicides*, ed. H. M. LeBaron, J. McFarland, O. Burnside and R. Clark, Elsevier Science, San Diego, 2008, pp. 13–29.
- P. Gamez and J. Reedijk, *Eur. J. Inorg. Chem.*, 2006, 29–42.
- D.-X. Wang, Q.-Y. Zheng, Q.-Q. Wang and M.-X. Wang, *Angew. Chem., Int. Ed.*, 2008, **47**, 7485–7488.
- B.-Y. Hou, Q.-Y. Zheng, D.-X. Wang, Z.-T. Huang and M.-X. Wang, *Chem. Commun.*, 2008, 3864–2866.
- D. W. P. M. Löwik and C. R. Lowe, *Eur. J. Org. Chem.*, 2001, 2825–2839.
- A. I. Vicente, J. M. Caio, J. Sardinha, C. Moiteiro, R. Delgado and V. Félix, *Tetrahedron*, 2012, **68**, 670–680.
- W. Maes and W. Dehaen, *Chem. Soc. Rev.*, 2008, **37**, 2393–2402.
- M.-X. Wang, *Chem. Commun.*, 2008, 4541–4551.
- M.-X. Wang, *Acc. Chem. Res.*, 2012, **45**, 182–195.
- L. J. Prins, P. Timmerman and D. N. Reinhoudt, *J. Am. Chem. Soc.*, 2001, **123**, 10153–10163.
- J. M. C. A. Kerckhoffs, M. G. J. ten Cate, M. A. Mateos-Timonedá, F. W. B. van Leeuwen, B. Snellink-Ruël, A. L. Spek, H. Kooijman, M. Crego-Calama and D. N. Reinhoudt, *J. Am. Chem. Soc.*, 2005, **127**, 12697–12708.
- G. Gattuso, G. Grasso, N. Marino, A. Notti, A. Pappalardo, S. Pappalardo and M. F. Parisi, *Eur. J. Org. Chem.*, 2011, 5696–5703.
- P. Comba, Y. D. Lampeka, L. Lötzbeier and A. I. Prikhod'ko, *Eur. J. Inorg. Chem.*, 2003, 34–37.
- M.-X. Wang and H.-B. Yang, *J. Am. Chem. Soc.*, 2004, **126**, 15412–15422.
- Q.-Q. Wang, D.-X. Wang, H.-W. Ma and M.-X. Wang, *Org. Lett.*, 2006, **8**, 5967–5970.
- D.-X. Wang and M.-X. Wang, *J. Am. Chem. Soc.*, 2013, **135**, 892–897.
- H.-B. Yang, D.-X. Wang, Q.-Q. Wang and M.-X. Wang, *J. Org. Chem.*, 2007, **72**, 3757–3763.
- W. Zhaoa, W. Wang, H. Changa, S. Cuia, K. Hua, L. Heb, K. Lub, J. Liuc, Y. Wuc, J. Qiand and S. Zhanga, *J. Chromatogr., A*, 2012, **1251**, 74–81.
- L. Wang, C. Yang, Q. Zhang, S. Wang, H. Lang, S. Zhang, W. Zhao and J. Zhang, *J. Sep. Sci.*, 2013, **36**, 2664–2671.
- P. Politzer, J. S. Murray and T. Clark, *Phys. Chem. Chem. Phys.*, 2013, **15**, 11178–11189.
- Y. Ma, K. Gross, C. Hollingsworth, P. Seybold and J. S. Murray, *J. Mol. Model.*, 2004, **10**, 235–239.
- J. S. Murray, K. E. Riley, P. Politzer and T. Clark, *Aust. J. Chem.*, 2010, **63**, 1598–1607.
- M. J. Frisch, G. W. Trucks, H. B. Schlegel, G. E. Scuseria, M. A. Robb, J. R. Cheeseman, G. Scalmani, V. Barone, B. Mennucci, G. A. Petersson, H. Nakatsuji, M. Caricato, X. Li, H. P. Hratchian, A. F. Izmaylov, J. Bloino, G. Zheng, J. L. Sonnenberg, M. Hada, M. Ehara, K. Toyota, R. Fukuda, J. Hasegawa, M. Ishida, T. Nakajima, Y. Honda, O. Kitao, H. Nakai, T. Vreven, J. A. Montgomery Jr., J. E. Peralta, F. Ogliaro, M. Bearpark, J. J. Heyd, E. Brothers, K. N. Kudin, V. N. Staroverov, R. Kobayashi, J. Normand, K. Raghavachari, A. Rendell, J. C. Burant, S. S. Iyengar, J. Tomasi, M. Cossi, N. Rega, J. M. Millam, M. Klene, J. E. Knox, J. B. Cross, V. Bakken, C. Adamo, J. Jaramillo, R. Gomperts, R. E. Stratmann, O. Yazyev, A. J. Austin, R. Cammi, C. Pomelli, J. W. Ochterski, R. L. Martin, K. Morokuma, V. G. Zakrzewski, G. A. Voth, P. Salvador, J. J. Dannenberg, S. Dapprich, A. D. Daniels, Ö. Farkas, J. B. Foresman, J. V. Ortiz, J. Cioslowski and D. J. Fox, *Gaussian 09 (Revision A.1)*, Gaussian, Inc., Wallingford, CT, 2009.
- I. R. Thomas, I. J. Bruno, J. C. Cole, C. F. Macrae, E. Pidcock and P. A. Wood, *J. Appl. Crystallogr.*, 2010, **43**, 362–366.
- Q.-Q. Wang, D.-X. Wang, Q.-Y. Zheng and M.-X. Wang, *Org. Lett.*, 2007, **9**, 2847–2850.
- P. Gans, A. Sabatini and A. Vacca, *Talanta*, 1996, **43**, 1739–1753.
- W. L. F. Armarego and C. L. L. Chai, *Purification of Laboratory Chemicals*, Butterworth Heinemann, Burlington, 2003.

- 28 G. Schwarzenbach and H. Flaschka, *Complexometric Titrations*, Methuen & Co, London, 1969.
- 29 Z. D. Hill and P. MacCarthy, *J. Chem. Educ.*, 1986, **63**, 162–167.
- 30 Bruker *SAINT-plus*, Bruker AXS Inc., Madison, Wisconsin, USA, 2007.
- 31 G. M. Sheldrick, *SADABS*, University of Göttingen, Germany, 1996.
- 32 G. M. Sheldrick, *Acta Crystallogr.*, 2008, **A64**, 112–122.
- 33 PyMOL Molecular Graphics System, Version 1.2r2, 2009, DeLano Scientific LLC.
- 34 F. A. Bulat, A. Toro-Labbé, T. Brinck, J. S. Murray and P. J. Politzer, *J. Mol. Model.*, 2010, **16**, 1679–1691.
- 35 F. A. Bulat and A. Toro-Labbe, unpublished.